Journal of Colloid and Interface Science 418 (2014) 140–146

Contents lists available at ScienceDirect

Journal of Colloid and Interface Science

www.elsevier.com/locate/jcis

Adsorption of Aerosol-OT at the calcite/water interface – Comparison of the sodium and calcium salts

Isabella N. Stocker [a], Kathryn L. Miller [a], Rebecca J.L. Welbourn [a], Stuart M. Clarke [a,*], Ian R. Collins [b], Christian Kinane [c], Philipp Gutfreund [d]

[a] BP Institute and Department of Chemistry, University of Cambridge, Madingley Rise, Madingley Road, Cambridge CB3 0EZ, UK
[b] BP Exploration Operating Company Ltd., Chertsey Road, Sunbury on Thames TW16 7LN, UK
[c] ISIS, Rutherford Appleton Laboratory, Harwell Science and Innovation Campus, Didcot, UK
[d] Institut Laue-Langevin, 6 rue Jules Horowitz, BP 156, 38042 Grenoble Cedex 9, France

ARTICLE INFO

Article history:
Received 31 August 2013
Accepted 18 November 2013
Available online 4 December 2013

Keywords:
Calcite
Calcium carbonate
Neutron reflection
AOT
Aerosol-OT

ABSTRACT

The adsorption of the surfactant Aerosol-OT (AOT) at the calcite–water interface has been investigated using batch adsorption isotherms and neutron reflection. The adsorption isotherms showed that NaAOT adsorption followed S-type adsorption behaviour with a maximum surface excess of 2.5 mg m^{-2} but the method could not be used for the investigation of $Ca(AOT)_2$ adsorption owing to the changes in the bulk phase behaviour of the solution. The surface excess, determined by neutron reflection at the critical micelle concentration (CMC), was 2.5 mg m^{-2} for $Ca(AOT)_2$ and 1.8 mg m^{-2} for NaAOT. The time dependence of the NaAOT adsorption suggests a slow conversion from the sodium to the calcium salt of AOT at the calcite–water interface by binding calcium ions released from the slightly soluble calcite. The layer thickness in both cases was 35 Å which indicates adsorption as bilayers or distorted micelles. At higher concentrations of NaAOT (~10× CMC) adsorption of an AOT lamellar phase was evident from Bragg peaks in the specular reflection.

To our knowledge, this is the first time that adsorption of a surfactant at the calcite–water interface has been investigated by neutron reflection. The technique provided significant new insight into the adsorption behaviour of AOT which would not have been accessible using traditional techniques.

1. Introduction

Calcium carbonate, one of the world's most common minerals, is of utmost industrial importance for its uses as a mineral filler in paper, in lubrication or in the cement and building industries, to name just a few. In these applications, calcium carbonate is used in a mixture with various organic compounds. Hence, the adsorption of organic compounds to calcium carbonate has been researched extensively [1–5]. Previously, such research has been limited to techniques like depletion isotherms, thermogravimetric analysis and ellipsometry [1,3,6]. Neutron reflection is a powerful technique in the study of interfaces. The large penetration depth of neutrons enables the investigation of buried interfaces with molecular resolution in the direction of the surface normal. In a recent paper we have demonstrated the applicability of the method of neutron reflection to the calcite–liquid interface, overcoming the challenges of surface roughness, cleanliness, dissolution and fragility of the crystals [7–9]. Here, the technique was used to study the adsorption of the industrially relevant surfactant Aerosol® OT (sodium bis(2-ethylhexyl)sulfosuccinate, AOT). AOT is a branched dichain sulphonate surfactant; its structure is shown in Fig. 1. It is an excellent wetting and dispersing agent and has many industrial uses, including paint formulation, detergency and in the paper and textile industries. AOT readily exchanges its sodium counterion for multivalent cations, even when present in only small concentrations [10].

It has been reported that NaAOT adsorbs on calcium carbonate with a maximum surface excess of 2.4 mg m^{-2} (based on adsorption isotherms determined by the depletion method) [11]. This surface excess is consistent with the formation of a bilayer with an area per molecule of 60 $Å^2$, although the structure has not been measured directly [11]. However, neutron reflection has been used to determine the structure of both NaAOT and $Ca(AOT)_2$ at the interfaces of water with air, silica and alumina [10,12–16]. At the

Abbreviations: AOT, Aerosol-OT; NaAOT, AOT sodium salt; $Ca(AOT)_2$, AOT calcium salt; CMC, critical micelle concentration; NRW, null-reflecting water; PCC, precipitated calcium carbonate; TOC, total organic carbon analysis.

* Corresponding author. Fax: +44 (0) 1223 765 701.
E-mail address: stuart@bpi.cam.ac.uk (S.M. Clarke).

0021-9797
http://dx.doi.org/10.1016/j.jcis.2013.11.046

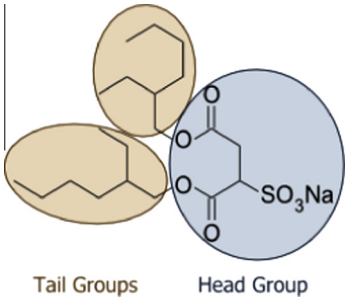

Fig. 1. Molecular structure of NaAOT.

interface of water with air and hydrophobic silica NaAOT was shown to adsorb as a monolayer of 18 Å thickness (the length of a fully extended molecule) with a surface excess of 0.9 mg m^{-2} at the CMC (2.5 mM for NaAOT) [10,13–16]. Investigation of the adsorption of $Ca(AOT)_2$ at the air–water interface revealed a similar structure at the CMC (0.4 mM for $Ca(AOT)_2$), with a layer thickness of 18 Å but higher surface excess of 1.0 mg m^{-2}. At the interface between hydrophilic sapphire and water, NaAOT adsorbs as a bilayer with a layer thickness of 41 Å and a surface excess of 2.6 mg m^{-2} at its CMC [12]. Adsorption of NaAOT lamellae was observed at the air–water and sapphire–water interfaces when the NaAOT concentration exceeded 22 mM, i.e. at concentrations where the isotropic micellar phase co-existed with the lamellar phase (L_1) [17–19].

In this paper, we present the adsorption of both the sodium and calcium salts of AOT on calcite as determined by batch adsorption isotherms and neutron reflection.

2. Neutron reflection

The details of the neutron reflection technique can be found elsewhere, e.g. [20]. Here the general approach is outlined. The geometry of a neutron reflection experiment is illustrated in Fig. 2.

The momentum transfer of specularly reflected neutrons, $\mathbf{q_z}$, is defined by

$$\mathbf{q_z} = \mathbf{k_f} - \mathbf{k_i}$$

$$|\mathbf{q_z}| = \frac{4\pi \sin\theta}{\lambda}$$

$\mathbf{k_i}$ and $\mathbf{k_f}$ are the wave vectors of incident and reflected neutrons respectively and λ is the wavelength.

Neutron reflection can be treated in an analogous way to the reflection of visible light. The neutron refractive index of non-absorbing materials can be defined as:

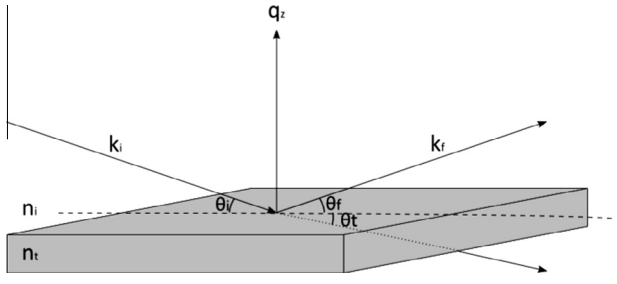

Fig. 2. In specular reflection, of interest here, the incident angle θ_i is equal to the reflected angle θ_f and the scattering is elastic. n_i and n_t are the refractive indices of the incident and transmitted media respectively. θ_i is the angle of transmission. k_i and k_f are the wave vectors of incident and reflected neutrons respectively and q_z is momentum transfer of specularly reflected neutrons. Specular reflection provides insight into the structure normal to a surface.

$$n = 1 - \frac{\lambda^2 \rho}{2\pi}$$

where ρ is the scattering length density of the material, essentially the variable that identifies how strongly a component scatters neutrons. It is defined as

$$\rho = \frac{\sum b_{coh}}{v_M}$$

where v_M is the molecular volume and $\mathbf{b_{coh}}$ the coherent scattering length, a nuclear property that varies across the periodic table and between isotopes.

Neutron reflectivity data analysis usually relies on fitting the calculated reflectivity profile from a model structure of the interface to the experimental data. The calculated reflectivity is compared to the experimental data and structural parameters varied until a best fit between calculated and experimental data is obtained. In the optical matrix method the interface is divided into layers with defined thickness and composition [21]. Reflection is considered from each interface and the reflectivity determined from interference of all reflected signals. Each layer can be represented by a characteristic matrix:

$$C_i = \begin{pmatrix} e^{i\beta_i} & r_{i,i+1}e^{i\beta_i} \\ r_{i,i+1}e^{-i\beta_i} & e^{-i\beta_i} \end{pmatrix}$$

where $\beta_i = \frac{2\pi}{\lambda} n_i d_i \sin\theta_i$, represents the phase change of the radiation passing through the layer, and $r_{i,i+1}$ is the reflection Fresnel coefficient of the interface between layers i and $i+1$.

$$r_{ij} = \frac{(p_i - p_j)}{(p_i + p_j)} \cdot e^{-0.5^* q_i^* q_i^* \sigma_{ij}^2}$$

where $p_i = n_i \sin(\theta_i)$, $q_i = \frac{4\pi}{\lambda} n_i \sin(\theta_i)$ and σ_{ij} is the Gaussian roughness of the ij interface.

The reflection from a stack of layers is given by the product of the layer matrices.

$$\begin{pmatrix} a & b \\ c & d \end{pmatrix} = C_0.C_1.C_2.C_3 \ldots C_n = \prod_0^n C_i$$

The reflected signal is given by $\frac{c.c^*}{a.a^*}$.

3. Materials and methods

Precipitated calcium carbonate (PCC) (Multifex-MM®) for batch adsorption isotherms was obtained from Specialty Minerals Inc. The crystal habit was calcite with a rhombohedral particle shape, an average particle size of 70 nm and a specific surface area of 17 $m^2 g^{-1}$ (information supplied by the manufacturer and verified by electron microscopy and nitrogen BET isotherm).

Calcite single crystals for neutron reflection were purchased from P&S Calcite Export Ltd. and cut and polished by Crystran Ltd. to a size of 45 × 45 × 15 mm^3, exposing the stable (104) face with a roughness of 8.5 ± 1 Å [7]. Crystals were cleaned by rinsing in turn with 20 mL methanol, 20 mL heptane (both obtained from Sigma-Aldrich, UK), 30 mL 18.2 MΩ deionised water pre-saturated with calcium carbonate (Multifex as above) and again 20 mL methanol. In a final step, they were cleaned by UV/ozone treatment for 15 min using a ProCleaner™ Plus (Bioforce Nanoscience). The samples were mounted in specifically designed sample cells immediately after UV/ozone treatment. The cells are described in more detail elsewhere [9].

NaAOT (Sigma, ⩾99% purity) was purified by liquid–liquid extraction as described by Li et al. [16]. The purity was confirmed from the absence of a minimum in the surface tension curve. $Ca(AOT)_2$ was prepared using the method proposed by Eastoe et al. [22]. Hereby a 1 M solution of purified NaAOT in ethanol

(Sigma–Aldrich, ⩾99.8%) was mixed with a saturated aqueous solution of $CaCl_2$ (as dihydrate, Sigma–Aldrich, ⩾99%). $Ca(AOT)_2$ was extracted with diethyl ether (Sigma–Aldrich, ⩾99.9%) and washed repeatedly until addition of $AgNO_3$ (Riedel-de Haën, ⩾99.5%) to the aqueous phase no longer produced cloudiness. The purity was assessed by surface tension and elemental analysis.

The samples for adsorption isotherms were prepared using the batch method. Hereby, various concentrations of adsorbate were added to fixed volumes of a calcite dispersion. Homogeneity between samples was ensured by shearing the stock dispersion using a Silverson L4R mixer. The surface excess of the adsorbate was determined using the depletion method. The concentration of the solute was determined after 24 h of equilibration by total organic carbon analysis (TOC) using a GE InnovOX TOC analyser. The surface excess could then be calculated from the difference between known initial and measured final concentrations.

Neutron Reflection measurements were performed at the instruments D17 at the Institut Laue-Langevin, France and CRISP at ISIS, U.K. Detailed description of the instruments can be found elsewhere [23,24]. Null reflecting water (NRW), i.e. water contrast matched to the calcite substrate contained a mixture of D_2O and H_2O in the ratio 0.78:0.22 v/v.

X-ray reflection measurements were performed at the beamline I07 at Diamond Lightsource, U.K.

4. Results

4.1. Adsorption isotherms determined by TOC

The adsorption isotherm of NaAOT on PCC at a pH of 8.4 ± 0.1 is shown in Fig. 3. The isotherm was found to be of sigmoidal type (S-type) [25]. No adsorption was observed below a concentration of 0.2 mM (∼CMC/10). Adsorption then started to rise sharply up to an equilibrium concentration of approximately 1.0 mM (∼CMC/2) where it levelled out to a plateau. The surface excess at the plateau was 2.5 ± 0.2 mg m^{-2}. Assuming formation of a double layer, this corresponds to an area per AOT moiety of 60 $Å^2$. Visual inspection of the samples showed that the solid calcite particles of the four samples with the lowest concentrations settled immediately after agitation, whereas the three samples with the highest concentrations (found near or at the adsorption plateau) were stable for several hours after agitation.

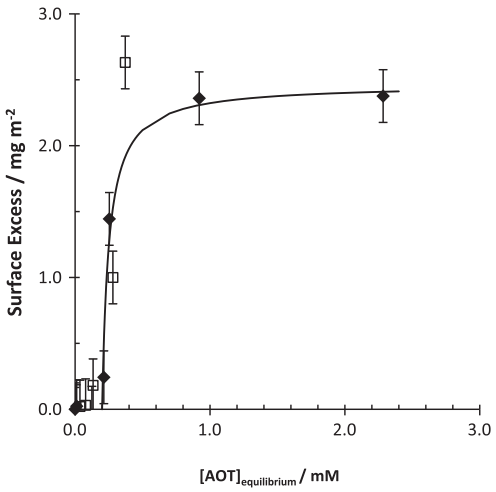

Fig. 3. Adsorption isotherm of NaAOT (circles) and $Ca(AOT)_2$ (squares) on calcite from water at 0.5% w/w solid content. Note the concentration plotted is that of the AOT anion.

The depletion of $Ca(AOT)_2$ was qualitatively similar to that of NaAOT at equilibrium concentrations below 0.3 mM. No $Ca(AOT)_2$ was adsorbed up to a concentration of 0.04 mM. For concentrations of 0.04–0.3 mM, adsorption occurred to a similar degree as observed for NaAOT. At higher equilibrium concentrations, $Ca(AOT)_2$ was mostly present as lamellar phase and could not be separated from the solid after equilibration. It was therefore impossible to determine equilibrium concentrations higher than 0.3 mM and hence the adsorption of $Ca(AOT)_2$ using the depletion method. The dispersion stability was similar to that observed for NaAOT, with the first five samples settling immediately after agitation, and the last four samples being stable for several hours.

4.2. AOT adsorption at its CMC determined by neutron and X-ray reflection

The structure of NaAOT and $Ca(AOT)_2$ at the calcite/water interface has been investigated by neutron reflection on the 3 different crystals C-Nai (i = 1,2) and C-Ca. All crystals showed good cleanliness (no reflected signal in NRW) with roughnesses in the range of 11–30 Å. The adsorption of NaAOT at its CMC of 2.5 mM was investigated on crystals C-Nai (i = 1–3) after different equilibration times; the neutron reflectivity profiles are shown in Fig. 4. In all cases the neutron reflectivity profile of the bare calcite/D_2O interface is shown for comparison. The increased reflected signal compared to the bare crystal is indicative of an adsorbed layer. The adsorbed NaAOT layer could always be fitted using a uniform single layer model with a layer thickness of 35 Å. However, the degree of solvent penetration varied between samples which suggests a different extent of adsorption. The fitting parameters are summarised in Table 1. Notably, the surface excess increased with equilibration time from 1.2 ± 0.1 mg m^{-2} after 2 h exposure to 1.8 ± 0.1 mg m^{-2} after 50 h exposure.

A separate crystal (C-Na3) was investigated by X-ray reflection in the presence of NaAOT at its CMC in H_2O after 18 h exposure; the results are shown in Fig. 1. A pronounced difference in reflected intensity is discernible at $q > 0.025$ $Å^{-1}$. The substrate roughness was 11.2 ± 0.5 Å and the adsorbed layer could be fitted with a similar uniform layer model (35 Å thickness, 1.9 ± 0.4 mg m^{-2} surface excess) with the fitting parameters given in Table 1.

The neutron reflectivity profile of C-Ca1 at the bare interface and in the presence of 0.4 mM $Ca(AOT)_2$ in the contrast of D_2O is shown in Fig. 6. The reflectivity in the presence of the surfactant was markedly higher over the entire q-range (excluding the critical edge and background). A smearing out of the critical edge is noticeable and can be attributed to small angle scattering by $Ca(AOT)_2$ micelles. The surfactant layer could be fitted as a uniform layer of 35 Å thickness (as before) and a surface excess of 2.5 ± 0.4 mg m^{-2}. The fitting parameters are summarised in Table 1.

4.3. Adsorption of NaAOT lamellar phase determined by neutron reflection

NaAOT undergoes a transition from a purely micellar phase to a two-phase regime where the micellar phase coexists with the lamellar phase at a concentration of 29 mM (∼10× CMC) [26]. The presence of the NaAOT lamellar phase is evident by clouding of the solution.

C-Na1 has been exposed to a solution of 45 mM NaAOT and the reflectivity has been recorded in the three contrasts of D_2O, H_2O and NRW. The D_2O contrast, recorded after 1 h equilibration, was essentially identical to that in the presence of NaAOT at the CMC described above (not shown) and could be fitted using the same uniform layer model. The contrasts of H_2O and NRW, recorded after 48 and 68 h respectively, are shown in Fig. 7. In the contrast of NRW, Bragg peaks are clearly discernible at q-values of

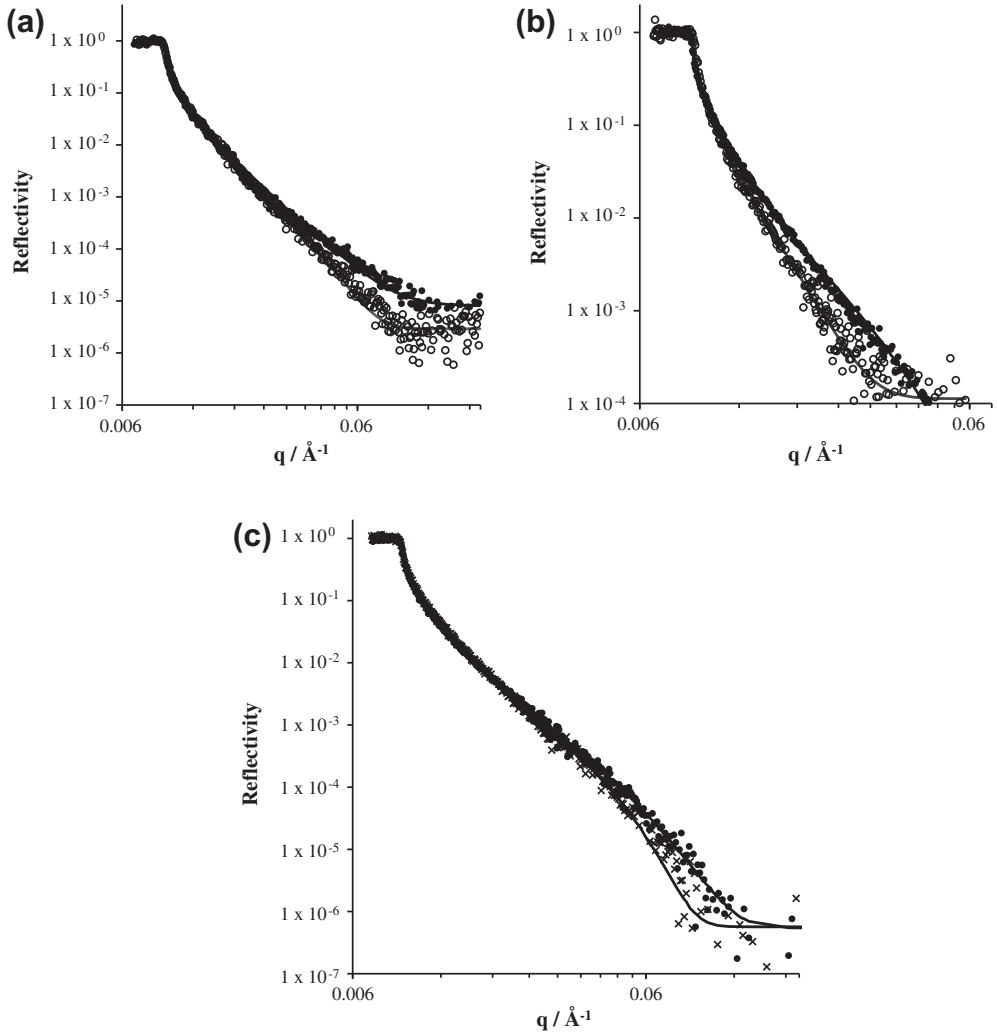

Fig. 4. Neutron reflectivity profiles from (a) C-Na1/D_2O interface: bare (white circles) and in the presence of 2.5 mM NaAOT (black circles) measured immediately (b) C-Na2/D_2O interface: bare (white circles) and in the presence of 2.5 mM NaAOT after 2 h exposure (black circles) and (c) C-Na2/D_2O interface in the presence of 2.5 mM NaAOT after 2 h (crosses) and 50 h exposure (black circles); figures (b) and (c) were split for clarity, solid lines represent fits to the data. Error bars omitted for clarity.

Table 1
Summary of fitting parameters in uniform single layer model which were used to fit the respective AOT layers adsorbed at the calcite/water interface.

	Contrasts	Equilibration time/h	Substrate roughness/Å	AOT layer			
				Thickness/Å	Roughness/Å	Surface excess/mg m^{-2}	Area per AOT moiety/$Å^2$
C-Na1 2.5 mM NaAOT	D_2O	1.5	19 ± 3	35 ± 3	5 ± 2	1.2 ± 0.1	124 ± 15
C-Na2 2.5 mM NaAOT	D_2O	2	30 ± 4	35 ± 3	17 ± 3	1.5 ± 0.2	100 ± 19
C-Na2 2.5 mM NaAOT	D_2O, H_2O, NRW	50	28 ± 1	35 ± 2	23 ± 4	1.8 ± 0.1	82 ± 6
C-Na3 2.5 mM NaAOT	H_2O (by XRR)	5	11.2 ± 0.5	35 ± 5	25 ± 1	1.9 ± 0.4	86 ± 27
C-Ca1 0.4 mM $Ca(AOT)_2$	D_2O	4	20 ± 3	35 ± 3	18 ± 5	2.5 ± 0.4	61 ± 14

0.029 $Å^{-1}$ and 0.059 $Å^{-1}$. Bragg diffraction occurs from a periodic array at values of q where the Bragg condition $d = 2n\pi/q$ (d = spacing of the repeat unit, n = integer) is met. The presence of Bragg peaks at q-values in the sequence of q and $2q$ in the specular reflection of C-Na1/45 mM NaAOT/NRW implies the presence of a regularly spaced array with a spacing of 220 ± 10 Å at the interface and is consistent with adsorption of the lamellar phase of NaAOT. The H_2O and NRW contrasts were successfully fitted with a model that included adsorption of a bilayer directly at the interface (as at the CMC) and adsorption of at least three NaAOT lamellae. Table 2 summarises the best fit parameters for three to five adsorbed lamellae, although higher numbers were possible. In all cases the adsorbed lamellae consisted of a NaAOT bilayer of 40 ± 3 Å thickness and an interlamellar water layer of 180 ± 5 Å. The combined thickness of AOT bilayer and interlamellar water was 220 ± 8 Å, consistent with the position of the Bragg peaks in the specular reflectivity of the NRW contrast. The data could be fitted with a varying number of adsorbed lamellae, whereby the hydration of the AOT bilayer increased with the number of adsorbed lamellae.

5. Discussion

The adsorption isotherm of NaAOT on calcite was found to be of S-type [25]. The result presented here is in remarkable agreement with that reported by Saleeb: all features reported – no adsorption

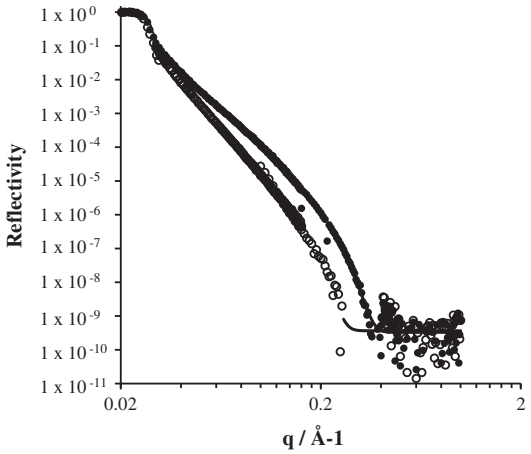

Fig. 5. X-ray reflectivity profiles from C-Na3/H_2O interface: bare (white circles) and in the presence of 2.5 mM NaAOT solution (black circles); solid lines represent fits to the data. Error bars omitted for clarity.

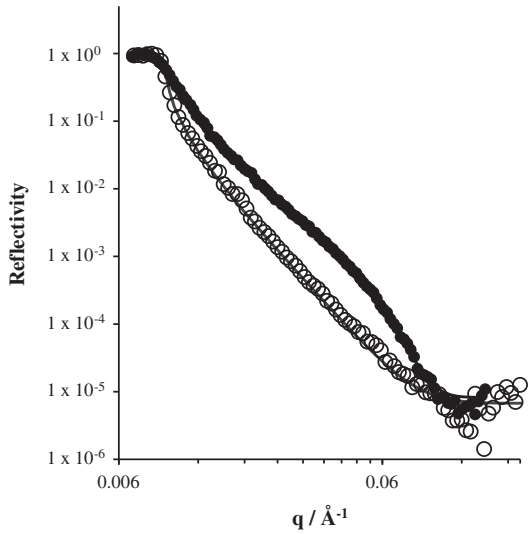

Fig. 6. Neutron reflectivity profile of C-Ca1/D_2O interface: bare (white circles) and in the presence of 0.4 mM $Ca(AOT)_2$ (black circles); solid lines represent fits to the data. Error bars omitted for clarity.

at very low concentration, a sharp rise in adsorption at a NaAOT concentration of 0.2 mM, and a plateau of 2.5 mg m^{-2} being reached at a concentration of 1.0 mM – were observed here as well [11]. The adsorption behaviour of NaAOT on calcite from water is typical for ionic surfactants adsorbing on a hydrophilic surface [27,28]. At very low concentrations, surfactants adsorb by ion exchange and adsorption levels are below the detection limit of the technique used here [29]. The ion exchange causes an increase in the local surfactant concentration so that self-assembly equivalent to micellisation in bulk solution can occur at the surface at concentrations significantly lower than the bulk CMC [27,28]. This 'surface micellisation' gave rise to the sharp increase in adsorption at a concentration of 0.2 mM (~CMC/10). At the subsequent adsorption plateau, the surface was saturated with respect to surfactant molecules so that no further adsorption could occur. The surface excess 2.5 mg m^{-2} is consistent with a close packed bilayer where each AOT moiety occupies an area of 61 $Å^2$. Such bilayer formation is expected on hydrophilic surfaces since termination by the hydrophobic tails would be unfavourable [27].

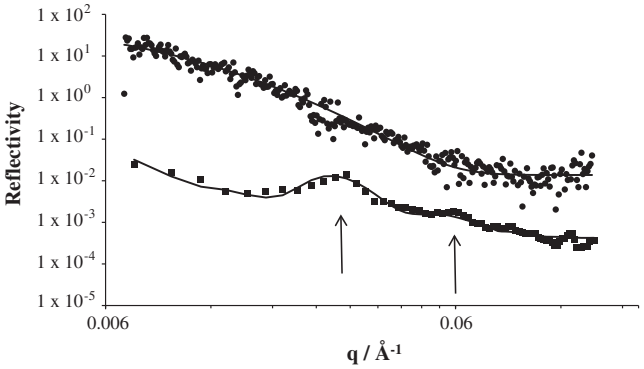

Fig. 7. Neutron reflectivity profiles of C-Na1 in the presence of 45 mM NaAOT in H_2O (circles) and NRW (squares); peaks at q = 0.029 and 0.059 $Å^{-1}$ in NRW contrast are Bragg peaks (highlighted by the arrows); solid lines are fit to the data. H_2O contrast has been shifted by factor of 1000 and error bars were omitted for clarity.

It was not possible to obtain an equivalent adsorption isotherm of $Ca(AOT)_2$ as the surfactant was depleted from solution by phase separation close to and above its CMC. While the adsorption plateau had not been reached for $Ca(AOT)_2$ at the experimentally accessible equilibrium concentrations, the steep rise in adsorption level coincides with that of NaAOT. However, unless multilayer formation occurs, the maximum surface excess must be similar to that of NaAOT as the NaAOT layer was already close packed at saturation. This assumption is further supported by the similar dispersion stability of the four highest concentrations of $Ca(AOT)_2$. This suggests that these four samples have similar adsorption levels and implies that the adsorption plateau had already been reached at an AOT concentration of 0.4 mM. It appears that at low AOT concentrations, the adsorption behaviour is independent of the counterion and that both NaAOT and $Ca(AOT)_2$ behave very similarly at this interface. Once adsorbed, NaAOT undergoes ion-exchange with Ca^{2+} from the calcite surface so that at equilibrium the adsorbed surfactant layer consists of $Ca(AOT)_2$ irrespective of which salt was used initially.

Conversely, the adsorption of NaAOT and $Ca(AOT)_2$ appeared to differ on calcite single crystals as evidenced by the differences in the neutron reflection data with NaAOT yielding a smaller surface excess than $Ca(AOT)_2$. The surface excess of $Ca(AOT)_2$ was 2.5 ± 0.4 mg m^{-2}, in good agreement with literature and the experimentally obtained adsorption isotherm [11]. NaAOT adsorbed to a lesser extent on calcite single crystals, with the surface excess ranging from 1.2 to 1.9 mg m^{-2} depending on exposure time; an increase in surface excess of NaAOT on calcite has been noted for increasing lengths of exposure as illustrated in Fig. 8. Unlike the samples for the batch adsorption isotherms, neutron reflection samples were not agitated during equilibration. Accordingly, the kinetics of Na/Ca cation exchange and adsorption are slower so that the surface excess was found to increase with exposure time.

We hypothesise that Na^+ ions co-adsorb with AOT during the initial stage of adsorption. As Ca^{2+} ions are released from the slightly soluble calcite surface the adsorbed NaAOT converts to $Ca(AOT)_2$. The presence of the divalent cation reduces the electrostatic repulsion between the charged head groups and a closer packing of the surfactant molecules is possible Even after 50 h the surface excess of NaAOT has not reached the same value that would be achieved if $Ca(AOT)_2$ was added directly, although it appears to have reached an equilibrium value of 1.8 mg m^{-2}. Given that the batch adsorption isotherms revealed a surface excess of 2.5 mg m^{-2} when NaAOT was used, it is plausible that a true equilibrium had simply not yet been reached over the course of the neutron reflection experiment and that much longer equilibration times are required in the absence of agitation.

Table 2
Summary of fitting parameters of C-Na1 in contact with 45 mM NaAOT in NRW and H_2O for three models with 3–5 adsorbed NaAOT lamellae, consisting of an NaAOT bilayer and an interlamellar water layer.

		3 Repeats	4 Repeats	5 Repeats
Substrate roughness/Å		20 ± 2	20 ± 2	20 ± 2
Directly adsorbed NaAOT				
	Solvent penetration/%	42 ± 2	42 ± 3	42 ± 3
	Thickness/Å	35 ± 2	35 ± 2	35 ± 2
	Roughness/Å	15 ± 1	15 ± 1	15 ± 1
Adsorbed lamellar phase – NaAOT layer				
	Solvent penetration/%	59 ± 2	64 ± 1	69 ± 2
	Thickness/Å	40 ± 3	40 ± 3	40 ± 3
	Roughness/Å	2 ± 0.5	2 ± 0.5	2 ± 0.5
Adsorbed lamellar phase – water layer				
	Thickness/Å	184 ± 5	185 ± 6	183 ± 5
	Roughness/Å	3 ± 0.5	2 ± 0.5	2 ± 0.5

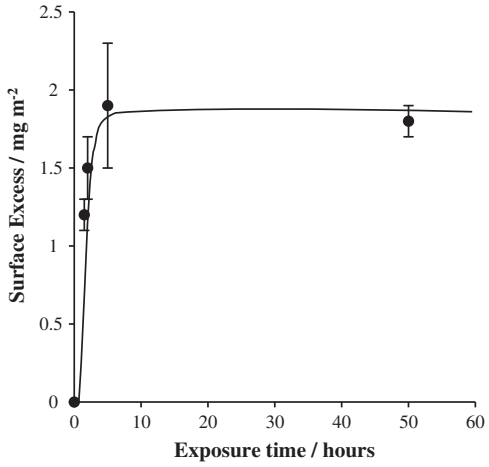

Fig. 8. Increasing surface excess of NaAOT at the calcite–water interface with exposure time; solid line is a guide to the eye.

The layer thickness was 35 Å in all cases. Taking into account the length of a single AOT molecule of 17 Å (calculated from geometrical considerations of the molecular structure), this layer thickness is consistent with a bilayer structure of extended AOT molecules or a layer of distorted micelles. An interdigitated bilayer structure, another structure commonly adopted by ionic surfactants, would have a layer thickness of 25 Å [27]. While such a structure was considered during data analysis it did not yield a good fit to the data. Since specular reflection has no lateral resolution, distinction between flattened micelles and extended bilayers is not possible by this technique. The reasonably high layer roughness of around 20 Å might be an indication that the structure consists of flattened micelles. However, additional experiments, such as atomic force microscopy, would be required to understand the adsorbed surfactant structure further. Here we conclude that AOT adsorbs either as extended bilayer or as distorted micelles at the calcite/water interface, as illustrated schematically in Fig. 9. The layer can be considered close packed in the case of $Ca(AOT)_2$, with an area of 61 ± 14 Å^2 per AOT moiety (122 ± 28 Å^2 per $Ca(AOT)_2$ molecule). Such close packing has already been reported for NaAOT at the sapphire/alumina interface (molecular area of 57 Å^2) [12]. The area per AOT moiety is larger for NaAOT (86 ± 14 Å^2 at apparent equilibrium), consistent with the greater electrostatic repulsion between charged head groups in the absence of the divalent Ca^{2+} counter ion.

The adsorption of the lamellar phase of NaAOT on calcite at a solution concentration of 45 mM was evident from off-specular reflection and the presence of Bragg diffraction peaks in the specular reflectivity profile. The calcite/water interface hence exhibits similar behaviour toward the NaAOT lamellar phase as the air/water, silica/water and sapphire/water interfaces [17,30]. The specular reflectivity is consistent with the adsorption of a NaAOT bilayer directly at the interface, as observed for NaAOT at its CMC, and the presence of at least three reasonably well aligned NaAOT lamellae. A schematic of the structure is shown in Fig. 10. A minimum of three lamellae were required to obtain a fit to the data but higher numbers lamellae were possible. Such an ambiguity in the data has been reported under similar conditions at the air/water interface [18].

Adsorption of the lamellar phase was found to be time dependent. This may be attributed to the relatively high viscosity of the solution [18]. No Bragg peaks were discernible in the contrast of D_2O recorded after 1 h of equilibration and the reflectivity was identical to that observed in the presence of NaAOT at the CMC. The H_2O contrast, measured after 48 h of exposure, is relatively

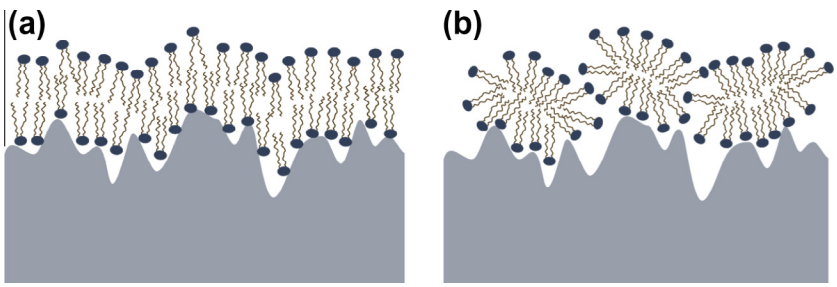

Fig. 9. Proposed structures of AOT adsorbed at calcite/water interface: (a) bilayer of AOT molecules or (b) distorted AOT micelles; surfactant tail groups (brown lines), head groups (blue circles), calcite (light blue), water not shown. (For interpretation of the references to colour in this figure legend, the reader is referred to the web version of this article.)

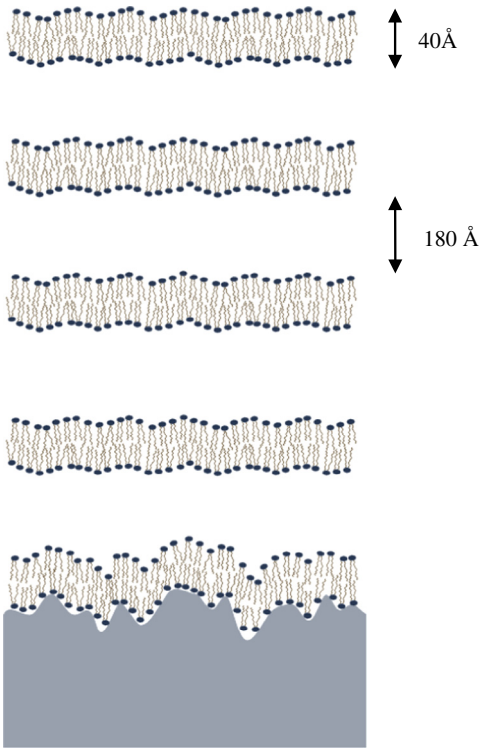

Fig. 10. Schematic representation of the NaAOT lamellar phase adsorbed at the C-Na1/water interface: one NaAOT bilayer adsorbed directly at calcite/water interface with 3–5 parallel aligned NaAOT lamellae consisting of a NaAOT bilayer and an interlamellar water layer.

insensitive to the presence of hydrogenous material so that the degree of adsorption at this stage is unknown. However, Bragg peaks were clearly evident in the contrast of NRW recorded after 68 h of equilibration. The lamellar spacing was 220 ± 10 Å. Since no further measurements could be made, it is unclear whether the structure after 68 h represents an equilibrium structure, and if so, at what point equilibrium had been reached. The lamellar spacing of 220 Å is slightly higher than in the bulk (210 Å), at the alumina/water interface (200 Å), at the silica/water interface (185 Å) and at the air/water interface (170 Å) at the same concentration and at room temperature. Addition of electrolyte has previously been reported to cause an increase in the lamellar spacing [30]. It is plausible that the increasing ionic strength, resulting from the continued dissolution of the calcite substrate, acts to destabilise the adsorbed lamellar phase, which would explain the larger lamellar spacing. The exchange of the AOT counterion from Na^+ to Ca^{2+} with time is also expected to change the composition of the lamellar phase and may be associated with a different lamellar spacing.

6. Conclusions

The adsorption of AOT has been monitored by batch adsorption isotherms and neutron reflection for both the sodium and calcium salts of the surfactant. The surface excess of 2.5 mg m^{-2} is consistent with a previous literature report [11]. Both salts were shown to form a 35 Å thick layer, consistent with an extended surfactant bilayer or distorted micellar structure. This structure has previously been reported on other hydrophilic substrates which suggests that AOT adsorption at the hydrophilic solid–water interface is reasonably independent of the nature of the surface [12]. The time dependence of NaAOT adsorption suggests that NaAOT converts to $Ca(AOT)_2$ at the calcite–water interface owing to the slight solubility of calcite. The adsorption of $Ca(AOT)_2$ could not be followed using traditional adsorption isotherms owing to the early onset of the lamellar phase which led to phase separation. Neutron reflection has provided unrivalled insight into the adsorbed structure of an important surfactant at a mineralogically significant surface. The methodology presented here has the scope to open up new areas of scientific interest that were previously inaccessible by traditional experimental techniques.

Acknowledgments

We thank BP plc. for financial support for this work, the ILL and ISIS staff and scientists for the allocation of beam time (RB920098, 9-12-257) and technical assistance with NR measurements.

References

[1] M.M. Thomas et al., Chem. Geol. 109 (1–4) (1993) 201–213.
[2] H.B. Abderrahmen et al., J. Chim. Phys. Phys. – Chim. Biol. 94 (4) (1997) 750–764.
[3] R.B. Bjorklund et al., Appl. Surf. Sci. 75 (1–4) (1994) 197–203.
[4] D.J. Cooke et al., Langmuir 26 (18) (2010) 14520–14529.
[5] N.I. Ivanova et al., Kolloidn. Zh. 49 (1) (1987) 148–150.
[6] R. Eriksson et al., J. Colloid Interf. Sci. 313 (1) (2007) 184–193.
[7] I.N. Stocker, et al. in: Adsorption at the Calcite–Liquid Interface with Molecular Precision, in: 16th European Symposium on Improved Oil Recovery, Cambridge, UK, 12–14th April, 2011; Cambridge, UK, 2011.
[8] I.N. Stocker, et al., Progress in Colloid and Polymer Science in press.
[9] I.N. Stocker, et al., in: UK Colloids 2011, Springer Berlin Heidelberg: vol. 139, pp. 91–99.
[10] Z.X. Li et al., Langmuir 13 (14) (1997) 3681–3685.
[11] F. Saleeb, Colloid Polym. Sci. 239 (1) (1970) 602–605.
[12] M.S. Hellsing et al., Langmuir 26 (18) (2010) 14567–14573.
[13] G. Fragneto et al., J. Colloid Interf. Sci. 178 (2) (1996) 531–537.
[14] Z.X. Li et al., Colloids Surf. A – Physicochem. Eng. Aspects 135 (1–3) (1998) 277–281.
[15] Z.X. Li et al., Trends Colloid Interf. Sci. IX 98 (1995) 243–247.
[16] Z.X. Li et al., J. Phys. Chem. B 101 (9) (1997) 1615–1620.
[17] M.S. Hellsing et al., Langmuir 27 (8) (2011) 4669–4678.
[18] Z.X. Li et al., Farad. Discuss. 104 (1996) 127–138.
[19] Z.X. Li et al., Langmuir 17 (19) (2001) 5858–5864.
[20] J. Penfold, R.K. Thomas, J. Phys.: Condens. Matter. 2 (6) (1990) 1369.
[21] O.S. Heavens, Optical Properties of Thin Solid Films, Butterworths Scientific Publications, London, 1955.
[22] J. Eastoe et al., J. Chem. Soc. Farad. Trans. 88 (3) (1992) 461–471.
[23] R. Cubitt, G. Fragneto, Appl. Phys. A: Mater. Sci. Process. 74 (2002) s329–s331.
[24] J. Penfold, Physica B 173 (1–2) (1991) 1–10.
[25] R.J. Hunter, Foundations of Colloid Science, Oxford University Press, Oxford, 2001. pp. 806.
[26] K. Fontell, J. Colloid Interf. Sci. 44 (2) (1973) 318–329.
[27] K. Holmberg et al., in: Surfactants and Polymers in Aqueous Solution, John Wiley & Sons, Ltd., 2003, pp. 357–387.
[28] M.J. Rosen, Surfactants and Interfacial Phenomena, third ed., Wiley-Blackwell, 2004.
[29] J.F. Scamehorn et al., J. Colloid Interf. Sci. 85 (2) (1982) 463–478.
[30] Z.X. Li et al., J. Phys. Chem. B 103 (49) (1999) 10800–10806.